Optical Properties of Plasmon-Tunable Tip Pyramids for Tip-Enhanced Raman Spectroscopy

Hudson Miranda, Cassiano Rabelo, Thiago L. Vasconcelos, Luiz Gustavo Cançado, and Ado Jorio*

For tip-enhanced Raman spectroscopy (TERS), the recently developed plasmon-tunable tip pyramid, composed of a gold micropyramidal body with a nanopyramid end, makes it possible to obtain spectral enhancements in 2D systems up to two orders of magnitude higher than what is found in the literature. Herein, the optical properties of these tips are explored, including the field-enhancement dependence on nanopyramid edge length (*L*), its apex diameter (*D*), tip–sample distance (*Z*), and the presence of a metallic micropyramid body. The study shown herein rationalizes the optical properties of these tips, important for understanding the related TERS results.

Apertureless tip-enhanced Raman spectroscopy (TERS) makes use of a nanoantenna to enable nano-Raman spectroscopy, i.e., to obtain the Raman spectra from samples with nanometric spatial resolution.[1–10] TERS in two-dimensional systems,[10] however, has to rely on ultra-high tip enhancements, so that the local near-field response, coming roughly from a circular area of 10 nm radius, overcomes the far-field signal obtained from the confocally illuminated surface area, which has a radius ranging roughly from 300 nm to 1 μm.

The recently developed plasmon-tunable tip pyramid (PTTP)[11] probe, composed of a gold micropyramidal body with a nanopyramid end (see **Figure 1**), has already shown to obtain TERS spectral enhancement (SE) on graphene one or even two orders of magnitude higher than what has been previously reported in the literature using other tips.[12] As an example of the PTTP's performance, **Figure 2** shows a micro-Raman (blue line) and a nano-Raman (red line) spectra obtained experimentally from a graphene sample. The SE observed for the *G* (1584 cm^{-1}) and 2*D* (2640 cm^{-1}) bands are over two orders of magnitude,

H. Miranda, Dr. C. Rabelo, Prof. L. G. Cançado, Prof. A. Jorio
Programa de Pós-Graduação em Engenharia Elétrica
UFMG
Belo Horizonte, MG 31270-901, Brazil
E-mail: adojorio@fisica.ufmg.br

Dr. T. L. Vasconcelos
Instituto Nacional de Metrologia, Qualidade e Tecnologia (Inmetro)
Duque de Caxias, RJ 25250-020, Brazil

Prof. L. G. Cançado, Prof. A. Jorio
Departamento de Física
UFMG
Belo Horizonte, MG 31270-901, Brazil

showing the very high local field enhancement performed by the PTTP, which is in resonance with the HeNe laser (λ = 632.8 nm).[11]

In this paper we explore the properties of PTTPs based on field simulations to better understand the tip properties, including the field-enhancement dependency on nanopyramid edge length (*L*), its apex diameter (*D*), and tip–sample distance (*Z*). We show that the metallic micropyramid body is crucial for the ultra-high enhancement obtained, and the study shown here rationalizes the optical properties of these tips, important for understanding TERS results.

The simulations presented here were conducted using the finite element method (FEM) in the frequency domain, as implemented by the Comsol Multiphysics V software. The boundaries were treated with a 600 nm-thick perfectly matched layer (PML). The gold material model utilized for the PTTP tip was obtained experimentally from reflection and transmission measurements of thin gold films, as reported by Johnson and Christy.[13] The tip illumination was configured as a tightly focused (N.A. = 1.4) radially polarized laser beam with wavelength λ = 632.8 nm, propagating toward the tip apex, as to properly mimic the back-scattering configuration of the experimental setup. The tip's geometry introduced in the simulation environment was consistent with the scanning electron microscopy (SEM) images of the PTTPs, such as the one shown in Figure 1. Both micropyramid and nanopyramid bodies were composed of gold. The micropyramid was truncated to fit the simulation environment and the nanopyramid's geometry was parameterized in terms of *D* and *L* to investigate the impact of the variables in the resulting electric field.

Figure 3 shows the dependence of the local fields on *L*, when the tips are illuminated from below (as in a conventional backscatter configuration based on an inverted microscope), with *D* = 40 nm. The color codes on panels numbered (I–IV) display the electric field module |*E*| for four different PTTPs. Three tips are in three different plasmonic resonance conditions (I, II, and IV), and one tip is out of resonance (III) with the laser. The graphic at the bottom shows the maximum field intensity (|*E*|^2) calculated 5 nm away from the tip apex for a range of *L* values (blue data stands for PTTPs, open black bullets will be discussed in the following paragraph). Interestingly, peak II, addressed to the second monopole mode of the plasmonic cavity resonance, is a condition that leads to a higher field intensity than the first mode (I peak). The large difference between peak II and peak III shows the effect of resonance.

ADVANCED
SCIENCE NEWS
www.advancedsciencenews.com
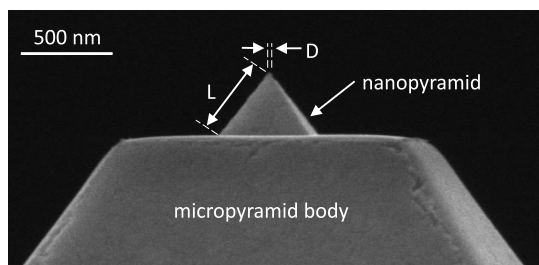
physica pss rrl
status solidi
www.pss-rapid.com

Figure 1. SEM image of the PTTP utilized to generate the TERS spectrum shown in Figure 2. L stands for the nanopyramid size on top of the micropyramidal body, and D stands for the tip apex diameter. The entire structure is composed of gold.
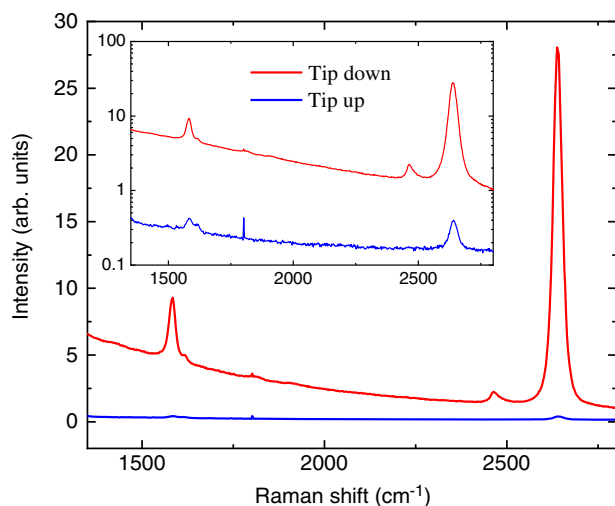

Figure 2. Micro-Raman and nano-Raman spectra of graphene on SiO_2 substrate. Micro-Raman (tip up, blue line) was obtained in a confocal backscattering geometry. The nano-Raman (tip down, red line) was obtained in a TERS configuration,[14–16] using a radially polarized HeNe laser beam with wavelength $\lambda = 632.8$ nm. The TERS tip was a PTTP[11] with nanopyramid size $L = 484$ nm and tip apex diameter $D = 25$ nm, as measured by SEM (see Figure 1). Spectra acquisition was five accumulations of 20 s each. The inset shows the same graphic in logarithmic scale.

Notice that this optimal L differs slightly from the value presented in a previous experimental study.[11] Two factors can account for the differences in optimal L. First, the simulations account for the optimization of the resonant excitation, whereas Stokes Raman scattering also has a resonance effect with red-shifted scattered light. Second, the optical properties of the surrounding air can produce shifts in plasmon resonance. Anyway, from now on the simulations consider the PTTP of highest calculated efficiency for the 632.8 nm HeNe laser illumination ($L = 425$ nm).

The black-open symbols connected by dashed lines in the graphic at the bottom of Figure 3 show the maximum field intensity ($|E|^2$) at the sample location, i.e., 5 nm below the tip's apex,[17] with the difference that we have now removed the micropyramidal body from the simulation, which was conducted considering only the nanopyramid. Here the values are
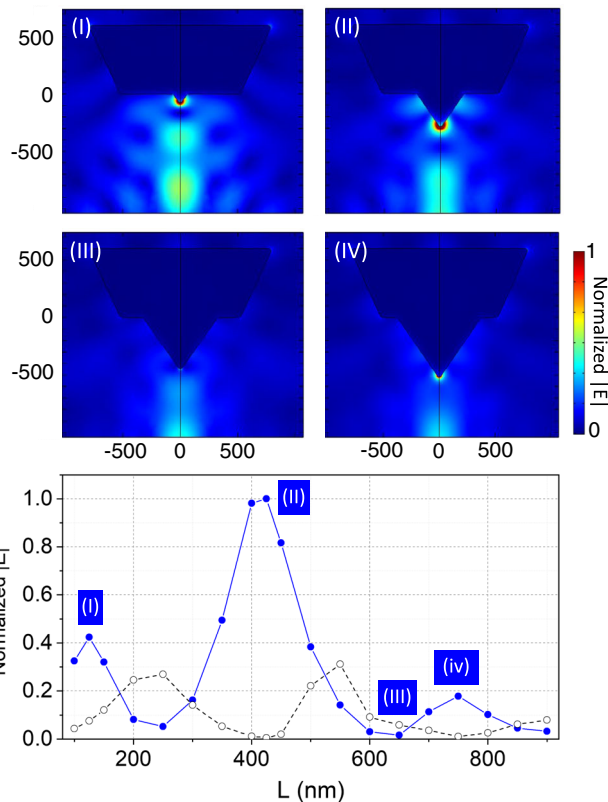

Figure 3. Electric field dependence on PTTP size L. I) $L = 125$ nm; II) $L = 425$ nm; III) $L = 650$ nm; and IV) $L = 750$ nm. The color code on panels numbered (I–IV) displays the electric field module $|E|$, all normalized to the highest value on tip (II). The graphic at the bottom displays the maximum field intensity ($|E|^2$) at the sample location, i.e., 5 nm below the tip's apex. Blue-solid bullets connected by blue lines are for the PTTP, whereas black-open bullets connected by dashed lines stand for nanopyramids without the micropyramid body. Both curves are normalized to the maximum value presented for II in the blue curve (with micropyramid body). For these simulations, tip apex diameters were fixed at $D = 40$ nm.

consistently normalized to the maximum value obtained for the PTTP with $L = 425$ nm, and the tip apex diameters were fixed at $D = 40$ nm. Comparing the results of the isolated nanopyramid with the PTTP data (blue curve), two important differences are evidenced. 1) The resonant peaks ($|E|^2$ maxima) shift in energy, because while for the PTTP resonances occur with plasmonic monopole modes (the metallic basis serve as a mirror), for the isolated nanopyramid, the resonances occur with plasmonic dipole modes.[11,18] 2) The maximum resonance value for the isolated nanopyramid (at $L \approx 550$ nm) drops to $\approx 30\%$ of the maximum resonance value for the PTTP (at $L \approx 425$ nm), showing the importance of the metallic plateau to the high TERS enhancements observed when using PTTPs. Notice that these effects are more relevant for TERS, where resonance with both incident and scattered light leads to $|E|^4$ field dependence.[8]

Figure 4 shows the dependence of the local fields on the PTTP apex diameter D. Panel (a) shows the variation of the electric field intensity $|E|^2$ within the sample plane, with the 0 nm position corresponding to the location exactly below the tip apex.
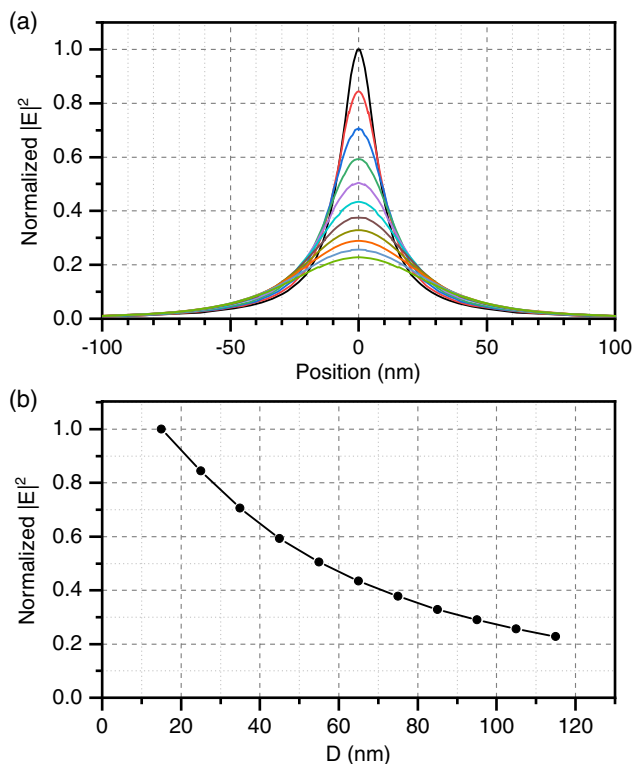
Figure 4. Electric field intensity $|E|^2$ dependence on PTTP tip apex diameter D. a) $|E|^2$ in the sample plane, where 0 nm position is below the tip apex. b) Plot of the maxima $|E|^2$ values obtained at 0 nm position. In (a,b) the tip apex diameter varies from $D = 15$ nm up to $D = 115$ nm, in steps of 10 nm. Here all nanopyramids have $L = 425$ nm.

From the highest peak value (black line) to the lowest peak value (green line), the tip apex diameter varies from $D = 15$ nm up to $D = 115$ nm, in steps of 10 nm. The field intensity drops to about 20% of the initial value when varying the tip from $D = 15$ to 115 nm.

The full-width at half maxima (FWHM) of the $|E|^2$ profiles in Figure 4a are related to the TERS spatial resolution. For the $D = 15$ nm tip, the FWHM = 18 nm, a value that is slightly above the tip diameter. For the $D = 115$ nm tip, the FWHM = 68 nm, a value considerably smaller than the tip's diameter. A more general discussion on the relation between the tip diameter and TERS resolution can be found in a previous study.[19]

Figure 5 shows the local field dependence on the tip–sample distance Z. The solid line corresponds to $|E|^2$ when moving the measurement point away from the tip but keeping the tip in the laser focus position. $Z = 0$ nm stands for the gold–air interface at the tip's apex. Bullets stand for $|E|^2$ at the sample plane when moving the tip out of focus, away from the sample position. For large values of Z, the bullets fall below the solid line because the tip effectively moves away from the focal position. However, these two simulations only show a considerably small deviation with $Z > 50$ nm, where the field intensity has already dropped by more than one order of magnitude. Therefore, within the near-field coupling range, moving the tip with respect to the laser focus is not an issue.

The data in Figure 5 are normalized to the value of $|E|^2$ 5 nm away from the sample plane, which is the nominal tip-sample
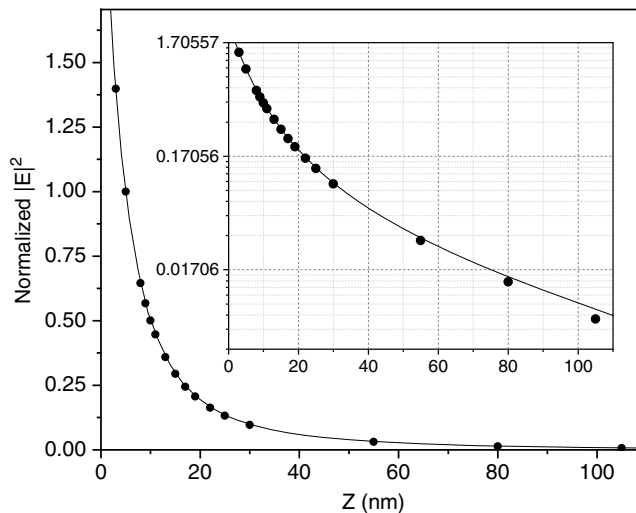

Figure 5. Electric field intensity $|E|^2$ dependence on tip–sample distance Z. Here the nanopyramid has $L = 425$ nm and $D = 40$ nm. The line stands for $|E|^2$ when moving literally away from the tip apex, keeping the tip in the laser focus, whereas bullets stand for $|E|^2$ at the sample plane when moving the tip out of focus, away from the sample position. The data are normalized to the value of $|E|^2$ 5 nm away from the sample plane.

working distance. Within this range, a 2 nm decrease in Z generates an almost 50% increase in $|E|^2$. Therefore, working closer to the sample, either by increasing the atomic force microscope's setpoint or by using scanning tunneling microscopy for tip–sample distance control, should significantly improve the TERS signal.

In summary, TERS enhancements in graphene up to two orders of magnitude higher than previous reports have been obtained utilizing resonant PTTPs.[11] We explored the dependence of the tip apex field on some geometrical factors. The field decreases significantly within the first 10–20 nm away from the tip apex. The size of the PTTP nanopyramid is responsible for tuning the plasmonic resonance with the excitation laser wavelength, and the presence of the micropyramid body, serving as an electronic reservoir, is crucial for the high enhancements. Smaller diameters of its apex provide higher enhancements and better spatial resolution. It is important to stress, however, that the connection between the tip apex diameter and the spatial resolution does not apply for tips working in high proximity, where gap plasmon is predominant, as for the ultra-high vacuum scanning tunneling microscopy-related TERS experiments.[20–22]

Acknowledgements

Conflict of Interest

The authors declare no conflict of interest.

[1] R. M. Stöckle, Y. D. Suh, V. Deckert, R. Zenobi, *Chem. Phys. Lett.* **2000**, *318*, 131.

[2] N. Hayazawa, Y. Inouye, Z. Sekkat, S. Kawata, *Opt. Commun.* **2000**, *183*, 333.

[3] L. Novotny, N. Van Hulst, *Nat. Photonics* **2011**, *5*, 83.

[4] B. Pettinger, P. Schambach, C. J. Villagómez, N. Scott, *Annu. Rev. Phys. Chem.* **2012**, *63*, 379.

[5] T. Schmid, L. Opilik, C. Blum, R. Zenobi, *Angew. Chem. Int. Ed.* **2013**, *52*, 5940.

[6] A. Taguchi, J. Yu, P. Verma, S. Kawata, *Nanoscale* **2015**, *7*, 17424.

[7] T. Deckert-Gaudig, A. Taguchi, S. Kawata, V. Deckert, *Chem. Soc. Rev.* **2017**, *46*, 4077.

[8] X. Shi, N. Coca-López, J. Janik, A. Hartschuh, *Chem. Rev.* **2017**, *117*, 4945.

[9] N. Kumar, B. M. Weckhuysen, A. J. Wain, A. J. Pollard, *Nat. Protocols* **2019**, *14*, 1169.

[10] F. Shao, R. Zenobi, *Anal. Bioanal. Chem.* **2019**, *411*, 37.

[11] T. L. Vasconcelos, B. S. Archanjo, B. S. Oliveira, R. Valaski, R. C. Cordeiro, H. G. Medeiros, C. Rabelo, A. Ribeiro, P. Ercius, C. A. Achete, A. Jorio, L. G. Cançado, *Adv. Opt. Mater.* **2018**, *6*, 1800528.

[12] R. Beams, L. G. Cançado, S. H. Oh, A. Jorio, L. Novotny, *Phys. Rev. Lett.* **2014**, *113*, 186101.

[13] P. B. Johnson, R. W. Christy, *Phys. Rev. B* **1972**, *6*, 4370.

[14] L. G. Cançado, A. Hartschuh, L. Novotny, *J. Raman Spectrosc.* **2009**, *40*, 1420.

[15] C. Rabelo, H. Miranda, T. L. Vasconcelos, L. G. Cançado, A. Jorio, *4th International Symposium on Instrumentation Systems, Circuits and Transducers (INSCIT 2019)*, IEEE, Sao Paulo, Brazil **2019**, pp. 35–40.

[16] H. Miranda, C. Rabelo, T. L. Vasconcelos, L. G. Cançado, A. Jorio, *4th International Symposium on Instrumentation Systems, Circuits and Transducers (INSCIT 2019)*, IEEE, Sao Paulo, Brazil **2019**, pp. 46–50.

[17] L. Novotny, B. Hecht, *Principles of Nano-Optics*, Cambridge University Press, Cambridge, UK **2012**.

[18] B. Archanjo, T. Vasconcelos, B. Oliveira, C. Song, F. Allen, C. Achete, P. Ercius, *ACS Photonics* **2018**, *5*, 2834.

[19] S. F. Becker, M. Esmann, K. Yoo, P. Gross, R. Vogelgesang, N. Park, C. Lienau, *ACS Photonics* **2016**, *3*, 223.

[20] R. Zhang, Y. Zhang, Z. Dong, S. Jiang, C. Zhang, L. Chen, L. Zhang, Y. Liao, J. Aizpurua, Y. Luo, J. L. Yang, J. G. Hou, *Nature* **2013**, *498*, 82.

[21] F. Benz, M. K. Schmidt, A. Dreismann, R. Chikkaraddy, Y. Zhang, A. Demetriadou, C. Carnegie, H. Ohadi, B. De Nijs, R. Esteban, J. Aizpurua, J. J. Baumberg, *Science* **2016**, *354*, 726.

[22] P. Roelli, C. Galland, N. Piro, T. J. Kippenberg, *Nat. Nanotechnol.* **2016**, *11*, 164.